Protective Action of Anandamide and its COX-2 Metabolite against L-Homocysteine-induced NLRP3 Inflammasome Activation and Injury in Podocytes

Guangbi Li, Min Xia, Justine M. Abais, Krishna Boini, Pin-Lan Li and Joseph K. Ritter

Department of Pharmacology and Toxicology

Virginia Commonwealth University School of Medicine, Richmond, VA

Running title: AEA and AEA Metabolites and NLRP3 Inflammasomes in Podocytes

Address correspondence to:

Dr. Joseph K. Ritter
Department of Pharmacology and Toxicology
Virginia Commonwealth University School of Medicine
1217 East Marshall Street, Room 531
Richmond, VA 23298
Tel: (804) 828-1022
Fax: (804) 828-0676
E-mail: jkritter@vcu.edu

Number of text pages: 28

Number of tables: 0

Number of figures: 8

Number of references: 68

Number of words in Abstract: 250

Number of words in Introduction: 595

Number of words in Discussion: 1277

Abbreviations: ASC, apoptosis-associated speck-like protein containing a caspase recruitment domain; AEA, anandamide; Ctrl, control; COX-2, cyclooxygenase-2; ESRD, end-stage renal disease; FF, folate-free; GDI, glomerular damage index; Hcys, L-homocysteine; hHcys, hyperhomocysteinemia; IL, interleukin; KO, knockout; LPS, lipopolysaccharide; NALP3, nucleotide-binding oligomerization domain-like receptor containing pyrin domain 3; ND, normal diet; NOD, nucleotide-binding oligomerization domain; PGE2-EA, prostaglandin E2-ethanolamide; VEGF, vascular endothelial growth factor; Vehl, vehicle; WT, wild-type.

Recommended section assignment: Gastrointestinal, Hepatic, Pulmonary, and Renal

ABSTRACT

Recent studies have demonstrated that L-homocysteine (Hcys)-induced podocyte injury leading to glomerular damage or sclerosis is attributable to the activation of the nucleotide-binding oligomerization domain-like receptor containing pyrin domain 3 (NLRP3) inflammasome. Given the demonstrated anti-inflammatory effects of endocannabinoids, the present study was designed to test whether anandamide (AEA) or its metabolites diminish NLRP3 inflammasome activation and prevent podocyte injury and associated glomerular damage during hyperhomocysteinemia (hHcys). AEA (100 µM) inhibited Hcys-induced NLRP3 inflammasome activation in cultured podocytes as indicated by elevated caspase-1 activity and interleukin-1β levels and attenuated podocyte dysfunction as shown by reduced vascular endothelial growth factor production. These effects of AEA were inhibited by the cyclooxygenase-2 (COX-2) inhibitor, celecoxib (CEL). In mice *in vivo,* AEA treatment attenuated glomerular NLRP3 inflammasome activation induced by hHcys accompanying a folate-free diet, based on inhibition of hHcys-induced colocalization of NLRP3 molecules and increased interleukin-1β levels in glomeruli. Correspondingly, AEA prevented hHcys-induced proteinuria, albuminuria, and microscopically observed glomerular damage. Hcys- and AEA-induced effects were absent in NLRP3-knockout mice. These beneficial effects of AEA against hHcys-induced NLRP3 inflammasome activation and glomerular injury were not observed in mice co-treated with CEL. We further demonstrated that prostaglandin E2 ethanolamide (PGE2-EA), a COX-2 product of AEA, at 10 µM had a similar inhibitory effect to that of 100 µM AEA on Hcys-induced NLRP3 inflammasome formation and activation in cultured podocytes. From these results, we conclude that AEA has anti-inflammatory properties, protecting podocytes from Hcys-induced injury by inhibition of NLRP3 inflammasome activation through its COX-2 metabolite, PGE2-EA.

3

Introduction

It has been well established that elevated serum homocysteine level, namely, hHcys, is associated with a wide range of diseases and pathological processes including neurological (Ravaglia et al., 2005; Bialecka et al., 2012; Perla-Kajan and Jakubowski, 2012), cardiovascular (Cavalca et al., 2001; Bialecka et al., 2012) and kidney disease (Wu et al., 2012), osteoporosis (McLean et al., 2004), and complications of aging (Yu et al., 2012). With respect to glomerulosclerosis and consequent end-stage renal disease (ESRD), a large body of evidence supports a pathogenic role of hHcys *via* its effects on extracellular matrix accumulation, mesangial expansion, podocyte injury, local oxidative stress and inflammation (Yi et al., 2007; Zhang et al., 2010; Li et al., 2013). Further mechanistic studies have recently demonstrated that the activation of NLRP3 inflammasomes is a triggering mechanism leading to podoycte injury and glomerular sclerosis during hHcys (Zhang et al., 2012; Han et al., 2013; Abais et al., 2014a; Xia et al., 2014). This type of inflammasome consists of NLRP3 protein, the adaptor molecule apoptosis-associated speck-like protein containing a caspase recruitment domain (ASC), and the cysteine protease, caspase-1, forming a cytosolic multiprotein complex that catalyzes the production of IL-1β, IL-18, and other products like high mobility group protein B1 (Martinon and Tschopp, 2005; Sutterwala et al., 2007). It is imperative to study whether this NLRP3 inflammasome can be a therapeutic target for prevention and treatment of glomerulosclerosis and ESRD during hHcys.

In previous studies, although endocannabinoids have been reported to have the proinflammatory role in the development of inflammation under certain pathological conditions (Vercelli et al., 2009; Gatta et al., 2012), there are numerous reports showing that endocannabinoids exert anti-inflammatory action in a variety of experimental models of

inflammatory disease including experimental hepatitis (Hegde et al., 2008), inflammatory bowel disease (Di Sabatino et al., 2011), lipopolysaccharide (LPS)-induced pulmonary inflammation (Berdyshev et al., 1998), nephropathy (Mukhopadhyay et al., 2010a; Mukhopadhyay et al., 2010b), and multiple sclerosis (Mestre et al., 2005). Among endocannabinoids, anandamide (AEA) has been documented to exert anti-inflammatory effects, but it has also been considered as a source of proinflammatory factors (Gatta et al., 2012). AEA can be metabolized by eicosanoid biosynthetic enzymes and therefore its role against inflammation may be associated with effects of its own and its metabolites on different inflammatory pathways (Turcotte et al., 2015). For example, COX-2 inhibition has been reported to block IL-2 release induced by AEA in mouse splenocytes and to prevent transcriptional activity of the IL-12p40 gene induced by AEA (Correa et al., 2008). Prostaglandin E2-ethanolamide (PGE2-EA), a COX-2-derived metabolite of AEA, attenuated cytokine-evoked epithelial damage in human mucosal explant colitis and reduced LPS-induced tumor necrosis factor-α production in monocytes (Brown et al., 2013). It is clear that AEA and its COX-2 metabolite, PGE2-EA, have potent anti-inflammatory effects. However, the molecular mechanism remains elusive by which AEA and its metabolites exert their anti-inflammatory action.

In the present study, we hypothesized that AEA and its metabolite may inhibit NLRP3 inflammasome activation in podocytes and thereby prevent glomerular inflammation and sclerosis during hHcys. To test this hypothesis, we first addressed whether AEA inhibits podocyte NLRP3 inflammasome formation and activation and prevents glomuerlar injury and sclerosis induced by hHcys *in vivo* in wild-type (WT) or *Nlrp3* gene knockout (KO) (*Nlrp3*$^{-/-}$) mice. *Nlrp3* knockout mice show resistance to hHcys-associated development of podocyte injury and glomerulosclerosis (Xia et al., 2014). We also determined whether COX-2 inhibition

ameliorates the beneficial effects of AEA. Then, we went on to examine whether PGE2-EA is the active metabolite of AEA that inhibits NLRP3 inflammasome activation and protects podocytes against Hcys-induced dysfunction and injury.

Materials and Methods

Cell Culture. Conditionally-immortalized mouse podocytes, kindly provided by Dr. Paul Klotman (Division of Nephrology, Department of Medicine, Mount Sinai School of Medicine, New York, NY), were cultured and maintained as described previously (Abais et al., 2013; Abais et al., 2014b). Briefly, they were grown at the permissive temperature (33°C) on collagen I-coated flasks or plates in RPMI 1640 medium supplemented with 10% fetal bovine serum and 10 U/mL recombinant mouse interferon-γ. The podocytes were then passaged and allowed to differentiate at 37°C for 10-14 days without interferon-γ before use in the experiments described below. Podocytes were treated with L-Hcys (40 μM, prepared in water) for 24 h, a dose and treatment time optimized in earlier studies.

Animals. Eight week-old male C57BL/6J WT and NLRP3 KO mice were used in the present study. To speed up the damaging effects of hHcys on glomeruli, all mice were uninephrectomized as described previously (Boini et al., 2011; Boini et al., 2012). This model has been demonstrated to induce glomerular damage unrelated to the uninephrectomy and arterial blood pressure, but specific to hHcys. After a 1-week recovery period from uninephrectomy, mice were fed either normal chow (ND) or folate-free (FF) diet (Dyets, Bethlehem, PA) for 4 weeks. At the same time, different groups of mice received AEA at 10 mg/kg/day with or without CEL at 2 mg/kg/day i.p. injection daily, which was based on some previous studies (DeMorrow et al., 2008; Zheng et al., 2008). All protocols involving animals

6

were approved by the Institutional Animal Care and Use Committee of Virginia Commonwealth University.

Immunofluorescence Microscopy. Double-immunofluorescence staining was performed using cultured podocytes grown on collagen-coated glass cover slips and frozen mouse kidney sections as described previously (Zhang et al., 2012; Abais et al., 2013; Abais et al., 2014b). Briefly, after fixation, the cells were incubated with goat anti-NLRP3 (Abcam, Cambridge, MA), followed by incubation with Alexa 488-labeled donkey anti-goat secondary antibody (1:200; Life Technologies, CA). Then, rabbit anti-ASC or rabbit anti-caspase-1 (1:100; Santa Cruz Biotechnology Inc, Santa Cruz, CA) was added to the cell slides and then incubated overnight at 4°C. To examine the distribution of F-actin fibers in podocytes, F-actin was stained with rhodamine–phalloidin (Invitrogen, Carlsbad, CA) for 15 min at room temperature as described previously (Abais et al., 2013). Frozen mouse kidney sections were fixed in acetone, blocked, then incubated with the same aforementioned primary antibodies overnight at 4 °C. Some coverslips with podocytes and frozen kidney sections were only stained for podocyte markers podocin (1:100; Sigma-Aldrich, St. Louis, MO) or desmin (1:100; BD Biosciences, San Jose, CA). Double immunofluorescent staining was performed by Alexa Fluor 488- or Alexa Fluor 555-labeled secondary antibody (1:200; Invitrogen) incubation for 1 h at room temperature. Slides were then washed, mounted, and observed using a confocal laser scanning microscope (Fluoview FV1000, Olympus, Tokyo, Japan). Image Pro Plus software (v. 6.0; Media Cybernetics, Bethesda, MD) was used to analyze colocalization, which was expressed as the Pearson correlation coefficient.

Caspase-1 Activity, IL-1β and vascular endothelial growth factor (VEGF) Measurements. Caspase-1 activity was measured by a commercially available colorimetric

7

assay (Biovision, Mountain View, CA), while IL-1β production and VEGF-A secretion were measured in the supernatant of cultured podocytes using an enzyme-linked immunosorbent assay (R&D System, Minneapolis, MN) according to the manufacturer's instructions.

Immunohistochemistry. Fixed kidney tissues were embedded in paraffin and 5 µm sections were cut. After heat-induced antigen retrieval, slides were washed with 3% hydrogen peroxide, blocked with control serum for 30 min, and then incubated with primary antibody diluted in phosphate-buffered saline containing 4% blocking serum. Anti-IL-1β (Abcam) antibody was used in this study. After incubation with primary antibody overnight, the sections were washed in phosphate-buffered saline and incubated with biotinylated IgG (1:200) for 1 hour and then with streptavidin-conjugated horse radish peroxidase for 30 min at room temperature. The peroxidase substrate, 3,3'-diaminobenzidine (50 µL), was added to each section and stained for 1 min. After washing, the slides were counterstained with hematoxylin for 5 min prior to mounting and imaging by light microscopy.

Urinary Protein and Albumin Measurements. Total urinary protein excretion was determined spectrophotometrically using the Bradford assay (Sigma-Aldrich), and urinary albumin excretion was measured using a commercially available mouse albumin enzyme-linked immunosorbent assay kit (Bethyl Laboratories, Montgomery, TX).

Glomerular Morphological Examinations. Fixed kidney tissues were paraffin-embedded, sectioned, and stained with periodic acid-Schiff. Glomerular morphology was observed and assessed semiquantitatively by light microscopy as described previously (Raij et al., 1984; Abais et al., 2014b).

Statistical analysis. All values are expressed as the mean ± S.E.M. Significant differences between multiple groups were examined using analysis of variance followed by post-hoc

analysis using the Student-Newman-Keuls test. A Chi-square test ($\chi 2$) test was used to assess the significance of ratio and percentage data. A p value $\leq$ 0.05 was considered statistically significant.

Results

Protective Action of AEA at Different Concentrations against Hcys-induced NLRP3 Inflammasome Activation and Injury via its COX-2 Metabolites in Cultured Podocytes. We first tested the effects of AEA at increasing concentrations up to 100 μM. As shown in Fig. 1A and B, AEA was found to have the significant inhibitory effects on Hcys-induced elevations in caspase-1 activity and IL-1β production in a concentration-dependent manner. Only at 100 μM was the inhibitory effect of AEA on NLRP3 inflammasome activation significant. When the podocytes were co-treated with the selective COX-2 inhibitor, CEL, the effects of AEA observed at high concentrations were completely blocked. As an indicator of Hcys-induced podocyte injury ((Boini et al., 2012; Zhang et al., 2012), Hcys markedly reduced the secretion of VEGF, and AEA at a concentration of 100 μM almost completely prevented this effect. In the presence of CEL, AEA failed to reverse Hcys-induced secretion of VEGF (Fig. 1C).

COX-2-dependent Protection of Glomerular Podocytes by AEA against hHcys-induced NLRP3 Inflammasome Formation and Activation in Mice *in Vivo*. We next examined whether AEA has protective effects against the formation and activation of NLRP3 inflammasomes in podocytes of mice with hHcys. After 4 weeks on a FF diet, all uninephrectomized mice developed hHcys with an average concentration of plasma Hcys level at 25 ± 3 μM, compared to 6 ± 2 μM in mice on the ND, even in *Nlrp3* gene KO mice (*Nlrp3*^{-/-}) (data not shown). As shown in Fig. 2A and 2B, confocal microscopic analysis showed the

9

formation of NLRP3 inflammasomes in glomeruli of wild-type (WT) mice with hHcys, as shown by increased colocalization of NLRP3 with ASC or caspase-1, but not in *Nlrp3*$^{-/-}$ mice. However, AEA given at 10 mg/kg/day i.p. over the time period of FF diet exposure substantially suppressed the increased colocalization of NLRP3 with ASC or caspase-1 in glomeruli of WT mice with hHcys. This AEA-mediated inhibitory effect on the assembly of NLRP3 inflammasomes during hHcys was completely blocked by CEL. The Pearson correlation coefficient data for colocalization of NLRP3 with ASC or caspase-1 is summarized in the bar graphs on the bottom of representative images. It is clear that the colocalization of NLRP3 with ASC or caspase-1 significantly increased in glomeruli of WT mice, but not in *Nlrp3*$^{-/-}$ on the FF diet. This increase in the formation of NLRP3 inflammasomes in glomeruli was not observed when they were treated with AEA, but it remained in mice treated with both AEA and CEL.

Correspondingly, the IL-1β level as an indicator of NLRP3 inflammasome activation was remarkably elevated in WT mice on the FF diet, but was not altered in mice on the ND, as shown in immunohistochemical stained photomicrographs (Fig. 2C). In the mice receiving AEA treatment or with *Nlrp3* gene deletion, however, the FF diet failed to increase the IL-1β level in glomerular podocytes. When these mice were administrated CEL, the effects of AEA treatment on the IL-1β increase during hHcys disappeared. CEL had no effect on the IL-1β level in the glomeruli of *Nlrp3*$^{-/-}$ mice no matter whether these mice received AEA or not. As shown in the bar graph of Fig. 2C, the increase in IL-1β level during hHcys was significantly attenuated only in the group of mice receiving AEA alone.

Prevention by AEA of hHcys-induced Glomerular Damage in Mice *in Vivo*. To determine whether AEA inhibition of NLRP3 inflammasome activation prevents glomerular injury in mice during hHcys, we analyzed changes in urinary protein and albumin excretion and morphological

integrity of glomeruli. Fig. 3A and B showed that WT mice on the FF diet had significant increases in urinary protein and albumin excretion compared to WT mice on the ND. In *Nlrp3*$^{-/-}$ mice, even with the FF diet, there were no changes in urinary protein and albumin excretion. In WT mice receiving AEA, urinary protein and albumin excretion had no changes during hHcys while those mice co-treated with AEA and CEL showed remarkable proteinuria and albuminuria. Morphologically, FF diet-fed WT but not *Nlrp3*$^{-/-}$ mice displayed glomerular pathology, characterized by increased extracellular matrix including collagen deposition, capillary collapse, and mesangial cell expansion (Fig. 3C). AEA treatment prevented these glomerular destructive changes induced by hHcys. In WT mice co-treated with AEA and CEL, however, the glomerular sclerotic changes remained profound. As shown in the bar graphs of Fig. 3C, the glomerular damage index (GDI) of FF diet-fed WT mice but not *Nlrp3*$^{-/-}$ mice was significantly increased. AEA treatment completely blocked the FF diet-induced increase in the GDI of WT mice, but AEA and CEL co-treatment had no effect on the increase in GDI by FF diet.

Amelioration by AEA of hHcys-induced Podocyte Injury in Mice. To further determine whether the protective effects of AEA against hHcys-induced glomerular damage associated with NLRP3 inflammasome activation are due to its actions on podocytes, we measured the expression levels of podocin and desmin, because reduction of podocin and increase in desmin indicate podocyte injury. Immunofluorescent microscopy demonstrated that FF diet-fed WT mice displayed marked decrease in podocin level and dramatic increase in desmin level, but ND-fed WT mice and all groups of *Nlrp3*$^{-/-}$ mice did not. In the FF diet-fed WT mice receiving AEA, however, there were no changes in the expression of both podocin (Fig. 4A) and desmin (Fig. 4B). The intensity analysis showed that except for the group of WT mice treated with AEA alone, all other groups of FF diet-fed WT mice had significantly decreased podocin and

11

increased desmin levels. AEA prevented podocyte injury in mice with hHcys, and COX-2 inhibition blocked its protective actions on podocytes.

Inhibition of Hcys-induced NLRP3 Inflammasome Formation by PGE2-EA in Cultured Podocytes. Given that the major product of AEA metabolism via COX-2 is PGE2-EA, we next tested whether PGE2-EA is protective against Hcys-induced formation and activation of NLRP3 inflammasome and injury in podocytes. By confocal microscopy, we examined whether PGE2-EA has effects on Hcys-induced NLRP3 inflammasome formation. As shown in Fig. 5, exposure of podocytes to Hcys (40 µM) significantly increased colocalization of NLRP3 with ASC (Fig. 5A) or caspase-1 (Fig. 5B). In the presence of PGE2-EA (10 µM), Hcys-enhanced colocalization of NLRP3 with ASC or caspase-1 in podocytes was substantially attenuated. However, co-treatment of podocytes with the same concentration of AEA (10 µM), the precursor to PGE2-EA, had no effect on Hcys-induced NLRP3 inflammasome formation. The Pearson correlation coefficient data for colocalization of NLRP3 with ASC or caspase-1 are shown in the bar graphs to the right of each representative image. Statistically, PGE2-EA was found to significantly inhibit Hcys-induced colocalization of NLRP3 with ASC or caspase-1, while AEA at the same concentration did not alter this Hcys-induced colocalization of the inflammasome components.

Blockade by PGE2-EA of Hcys-induced NLRP3 Inflammasome Activation in Cultured Podocytes. We also examined whether outcomes of Hcys-induced NLRP3 inflammasome activation in cultured podocytes can similarly be affected by PGE2-EA or AEA. Treatment with Hcys significantly increased caspase-1 activity as measured by microplate fluospectrometric analysis. Co-treatment of these podocytes with PGE2-EA (10 µM) almost abolished Hcys-induced increase in podocyte caspase-1 activity, but AEA co-treatment did not have such effect

(Fig. 6A). Similarly, the elevation in IL-1β level in culture medium of podocytes treated with Hcys was blocked by PGE2-EA but not by AEA at the same concentration (Fig. 6B).

Protective Effect of PGE2-EA against Hcys-induced Injury to Cultured Podocytes. To determine whether PGE2-EA prevents podocyte morphological changes and dysfunction associated with Hcys-induced NLRP3 inflammasome formation and activation, F-actin fiber arrangement and VEGF production in podocytes as structural and functional parameters were examined under different treatments. Immunofluorescent microscopy showed that Hcys resulted in loss of the distinct arrangement of F-actin fibers observed in control cells, as shown by their condensation at cell edges in fluorescent staining. This Hcys-induced rearrangement of F-actin fibers in podocytes was largely prevented by PGE2-EA co-treatment, but not by AEA. The intensity quantitation of F-actin fluorescent staining showed that Hcys-induced loss of F-actin in podocytes was significantly suppressed by PGE2-EA, but not by AEA at the same concentration (Fig. 7A). It was also found that Hcys markedly reduced VEGF secretion in podocytes and this reduction of VEGF secretion was substantially blocked by co-treatment with PGE2-EA, but not with AEA (Fig. 7B).

We also examined the effects of PGE2-EA on the expression of podocin and desmin to further evaluate its protective action on podocytes upon Hcys stimulation. Under basal condition, the cultured podocytes were found to highly express podocin. After treatment with Hcys, the podocin staining was significantly reduced, but such reduction was blocked by co-treatment of these cells with PGE2-EA. AEA co-treatment at the same concentration, however, had little apparent ability to block this Hcys-induced decrease in podocin. The intensity analysis showed that in podocytes co-treated with PGE2-EA, Hcys induced significantly less reduction of podocin expression (Fig. 8A) compared to control and AEA co-treated cells. In contrast, desmin was

found to be overexpressed in response to Hcys treatment. This Hcys-induced overexpression of desmin in podocytes was significantly decreased by PGE2-EA, but was not affected by AEA (Fig. 8B).

Discussion

The present study was designed to determine whether AEA or its COX-2 metabolite, PGE2-EA, can prevent hHcys-induced podocyte injury and glomerular damage through inhibition of NLRP3 inflammasome formation and activation. We demonstrated that AEA can suppress the activation of NLRP3 inflammasome and prevent podocyte injury and dysfunction associated with hHcys. However, the beneficial effects of AEA were blocked or attenuated by co-treatment with the selective COX-2 inhibitor, CEL. These results suggest that PGE2-EA is the active metabolite of AEA that inhibits NLRP3 inflammasome formation and activation and protects podocytes against Hcys-induced dysfunction and injury, preventing glomerular damage or sclerosis during hHcys.

Although endocannabinoids including AEA and its metabolites in some cases may produce proinflammatory actions, a large body of evidence supports potent anti-inflammatory actions in a variety of inflammatory diseases. For example, AEA has been reported to inhibit inflammatory responses in experimental hepatitis (Hegde et al., 2008), inflammatory bowel disease (Di Sabatino et al., 2011), LPS-induced pulmonary inflammation (Berdyshev et al., 1998), nephropathy (Mukhopadhyay et al., 2010a; Mukhopadhyay et al., 2010b), and multiple sclerosis (Mestre et al., 2005). Additional studies demonstrate that elevation of AEA levels by genetic knockout or chemical inhibition of the AEA degradative enzyme, fatty acid amide hydrolase,

ameliorates traumatic brain injury-induced neuronal inflammation and cystitis-associated pain sensation (Tchantchou et al., 2014; Wang et al., 2015). However, the mechanism by which endocannabinoids, in particular AEA, impart their anti-inflammatory effect remains poorly understood. Recent evidence suggests that aberrant activation of NLRP3 inflammasome, an intracellular inflammatory machinery, is involved in the development of different chronic degenerative diseases and pathological processes. Examples include diabetes mellitus (Masters et al., 2010; Grishman et al., 2012; Lee et al., 2013), obesity (Esser et al., 2013; Wang et al., 2014), silicosis (Peeters et al., 2013; Peeters et al., 2014), liver cirrhosis (Wree et al., 2014), and ESRD (Abais et al., 2014a; Abais et al., 2014b; Xia et al., 2014). The latter group of studies by our laboratory demonstrate that the formation and activation of the NLRP3 inflammasome contributes to glomerular injury from a sterile inflammatory response to hHcys. These studies led us to wonder whether AEA can inhibit hHcys-induced NLRP3 inflammasome activation and thereby prevents consequent podocyte injury and glomerular damage.

To test this hypothesis, we first examined the concentration-dependent inhibition by AEA of Hcys-induced NLRP3 inflammasome activation in podocytes. It was found that this endocannabinoid attenuated Hcys-enhanced caspase-1 activity and IL-1β production in a concentration-dependent manner, and that this effect of AEA to inhibit NLRP3 inflammasome activation was statistically significant at a concentration of 100 μM. Moreover, AEA was found to protect podocytes against Hcys-induced injury, as shown by normalization of VEGF production. The extrapolatability of this effect to the *in vivo* setting was investigated using mice with hHcys induced by a FF diet. AEA treatment significantly attenuated hHcys-induced NLRP3 inflammasome formation in glomeruli, as shown by reduced aggregation of inflammasome components by confocal microscopy. Consistent with inhibitory effects on

inflammasome formation, AEA also strongly inhibited increased IL-1β production resulting from the FF diet. Functional studies showed that hHcys-induced elevations of urinary protein and albumin were remarkably attenuated by AEA. Correspondingly, it was found that AEA prevented podocyte injury and mesenchymal cell expansion following hHcys-induced NLRP3 inflammasome activation by immunofluorescent staining and immunohistochemistry, respectively. To our knowledge, these results represent the first experimental evidence that AEA can abrogate podocyte damage associated with Hcys-induced NLRP3 inflammasome activation *in vivo*. Since podocyte injury is a critical step in the initiation and development of glomerular sclerosis or ESRD (Asanuma and Mundel, 2003), this protective effect of AEA on Hcys-induced NLRP3 inflammasome activation could represent a useful strategy for preventing the progression of glomerular injury during hHcys.

Several laboratories have reported inhibitory effects on inflammation and associated diseases and pathologic phenomena by elevating endogenous AEA levels through different approaches, including fatty acid amide hydrolase gene KO (Naidu et al., 2010; Kinsey et al., 2011; Wang et al., 2015), fatty acid amide hydrolase inhibitors (Kinsey et al., 2011; Schuelert et al., 2011; Booker et al., 2012; Caprioli et al., 2012; Kerr et al., 2012; Murphy et al., 2012; Sasso et al., 2012; Krustev et al., 2014; Salaga et al., 2014; Tchantchou et al., 2014), and AEA reuptake inhibitors (Mestre et al., 2005; D'Argenio et al., 2006). Further studies are needed to address whether such approaches are also protective in glomerular injury associated with hHcys. Our finding that exogenous AEA produces anti-inflammatory effects is consistent with several reports documenting beneficial effects of exogenous AEA in inflammatory disease models, such as liver damage (Hegde et al., 2008), LPS-induced pulmonary inflammation (Berdyshev et al., 1998), periodontitis (Rettori et al., 2012), hypoxia-ischemia injury (Lara-Celador et al., 2012),

delayed-type hypersensitivity (Jackson et al., 2014), and viral demyelinating disease (Hernangomez et al., 2012).

Since a recent report showed that COX-2 products of AEA exert protective effects against inflammation (Turcotte et al., 2015), we also investigated the role of COX-2 in the mechanism of AEA's protective effects against NLRP3 inflammasome activation and podocyte and glomerular injury from hHcys. The presence of the COX-2 inhibitor, CEL, attenuated the protective effects of AEA on markers of Hcys-induced NALP3 inflammasome activation and injury to cultured podocytes (Fig. 1), and it was also found to block or attenuate the protective *in vivo* effects of exogenous AEA on various indicators of hHcys-associated NALP3 inflammasome activation and sequelae (Figs. 2-4). Although these findings support the capacity of podocytes to metabolize AEA to PGE2-EA, the current study did not address this question directly. However, AEA is known to be present in the renal cortex including glomerular elements (Deutsch et al., 1997; Ritter et al., 2012) and podocytes express cyclooxygenases including COX-2 (Lemieux et al., 2003).

Next, we performed in vitro experiments to determine if the COX-2 product of AEA was active as an inhibitor of NLRP3 inflammasome activation. It has been well established that COX-2 metabolism of AEA leads to a diverse array of prostaglandin ethanolamides, including PGG2-EA, PGH2-EA, PGD2-EA, PGE2-EA, PGF2α-EA, and PGI2-EA (Yu et al., 1997; Kozak et al., 2002; Koda et al., 2004; Yang et al., 2005). In this regard, PGE2-EA, one of the most studied COX-2 metabolites of AEA, has been reported to inhibit inflammation in different disease models. Inhibition of IL-12p40 production by AEA acting on the promoter repressor element GA-12 was mimicked by PGE2-EA and was partially reversed by the selective COX-2 inhibitor, NS-398 (Correa et al., 2008). PGE2-EA has been demonstrated to reduce epithelial

17

damage evoked by pro-inflammatory cytokines, tumor necrosis factor-α and IL-1β, in an ex vivo human mucosal explant colitis model (Nicotra et al., 2013). Correspondingly, PGE2-EA was found to downregulate the production of tumor necrosis factor-α by human mononuclear cells in response to an immune stimulus, LPS-activated toll-like receptor 4 (Brown et al., 2013). Based on this information, we hypothesized that PGE2-EA may be the active COX-2 metabolite of AEA inhibiting NLRP3 inflammasome activation. Our results showed that PGE2-EA (10 µM) significantly inhibited the formation and activation of NLRP3 inflammasome and prevented podocyte injury in the presence of Hcys. In contrast, it was found that AEA (10 µM) had no significant effect on Hcys-induced NLRP3 inflammasome activation and podocyte injury. These results suggest that PGE2-EA is responsible at least in part for the inhibitory effects of AEA on NLRP3 inflammasome activation, preventing podocyte injury and glomerular damage during hHcys.

In summary, the present study demonstrates a novel anti-inflammatory role of AEA and, in particular, the COX-2 metabolite of AEA, PGE2-EA, on hHcys-induced NLRP3 inflammasome activation. This action of PGE2-EA is associated with inhibition of podocyte injury and glomerular damage during hHcys. These results may establish a new therapeutic strategy for hHcys-induced glomerular sclerosis by inhibition of NLRP3 inflammasome activation.

Authorship Contributions

Participated in research design: G. Li, Xia, Abais, Boini, P.-L. Li, and Ritter.

Conducted experiments: G. Li, Xia, Ritter.

Performed data analysis: G. Li, Xia, P.-L. Li, Ritter.

Wrote or contributed to the writing of the manuscript: G. Li, Xia, P.-L. Li, Ritter.

References

References

Abais JM, Xia M, Li G, Chen Y, Conley SM, Gehr TW, Boini KM and Li PL (2014a) Nod-like receptor protein 3 (NLRP3) inflammasome activation and podocyte injury via thioredoxin-interacting protein (TXNIP) during hyperhomocysteinemia. *J Biol Chem* **289**:27159-27168.

Abais JM, Xia M, Li G, Gehr TW, Boini KM and Li PL (2014b) Contribution of endogenously produced reactive oxygen species to the activation of podocyte NLRP3 inflammasomes in hyperhomocysteinemia. *Free Radic Biol Med* **67**:211-220.

Abais JM, Zhang C, Xia M, Liu Q, Gehr TW, Boini KM and Li PL (2013) NADPH oxidase-mediated triggering of inflammasome activation in mouse podocytes and glomeruli during hyperhomocysteinemia. *Antioxid Redox Signal* **18**:1537-1548.

Asanuma K and Mundel P (2003) The role of podocytes in glomerular pathobiology. *Clin Exp Nephrol* **7**:255-259.

Berdyshev E, Boichot E, Corbel M, Germain N and Lagente V (1998) Effects of cannabinoid receptor ligands on LPS-induced pulmonary inflammation in mice. *Life Sci* **63**:Pl125-129.

Bialecka M, Kurzawski M, Roszmann A, Robowski P, Sitek EJ, Honczarenko K, Gorzkowska A, Budrewicz S, Mak M, Jarosz M, Golab-Janowska M, Koziorowska-Gawron E, Drozdzik M and Slawek J (2012) Association of COMT, MTHFR, and SLC19A1(RFC-1) polymorphisms with homocysteine blood levels and cognitive impairment in Parkinson's disease. *Pharmacogenet Genomics* **22**:716-724.

Boini KM, Xia M, Abais JM, Xu M, Li CX and Li PL (2012) Acid sphingomyelinase gene knockout ameliorates hyperhomocysteinemic glomerular injury in mice lacking cystathionine-β-synthase. *PLoS One* **7**:e45020.

Boini KM, Xia M, Li C, Zhang C, Payne LP, Abais JM, Poklis JL, Hylemon PB and Li PL (2011) Acid sphingomyelinase gene deficiency ameliorates the hyperhomocysteinemia-induced glomerular injury in mice. *Am J Pathol* **179**:2210-2219.

Booker L, Kinsey SG, Abdullah RA, Blankman JL, Long JZ, Ezzili C, Boger DL, Cravatt BF and Lichtman AH (2012) The fatty acid amide hydrolase (FAAH) inhibitor PF-3845 acts in the nervous system to reverse LPS-induced tactile allodynia in mice. *Br J Pharmacol* **165**:2485-2496.

Brown KL, Davidson J and Rotondo D (2013) Characterisation of the prostaglandin E2-ethanolamide suppression of tumour necrosis factor-α production in human monocytic cells. *Biochim Biophys Acta* **1831**:1098-1107.

Caprioli A, Coccurello R, Rapino C, Di Serio S, Di Tommaso M, Vertechy M, Vacca V, Battista N, Pavone F, Maccarrone M and Borsini F (2012) The novel reversible fatty acid amide hydrolase inhibitor ST4070 increases endocannabinoid brain levels and counteracts neuropathic pain in different animal models. *J Pharmacol Exp Ther* **342**:188-195.

Cavalca V, Cighetti G, Bamonti F, Loaldi A, Bortone L, Novembrino C, De Franceschi M, Belardinelli R and Guazzi MD (2001) Oxidative stress and homocysteine in coronary artery disease. *Clin Chem* **47**:887-892.

Correa F, Docagne F, Clemente D, Mestre L, Becker C and Guaza C (2008) Anandamide inhibits IL-12p40 production by acting on the promoter repressor element GA-12: possible involvement of the COX-2 metabolite prostamide E(2). *Biochem J* **409**:761-770.

D'Argenio G, Valenti M, Scaglione G, Cosenza V, Sorrentini I and Di Marzo V (2006) Up-regulation of anandamide levels as an endogenous mechanism and a pharmacological strategy to limit colon inflammation. *Faseb j* **20**:568-570.

DeMorrow S, Francis H, Gaudio E, Venter J, Franchitto A, Kopriva S, Onori P, Mancinelli R, Frampton G, Coufal M, Mitchell B, Vaculin B and Alpini G (2008) The endocannabinoid anandamide inhibits cholangiocarcinoma growth via activation of the noncanonical Wnt signaling pathway. *Am J Physiol Gastrointest Liver Physiol* **295**:G1150-1158.

Deutsch DG, Goligorsky MS, Schmid PC, Krebsbach RJ, Schmid HH, Das SK, Dey SK, Arreaza G, Thorup C, Stefano G and Moore LC (1997) Production and physiological actions of anandamide in the vasculature of the rat kidney. *J Clin Invest* **100**:1538-1546.

Di Sabatino A, Battista N, Biancheri P, Rapino C, Rovedatti L, Astarita G, Vanoli A, Dainese E, Guerci M, Piomelli D, Pender SL, MacDonald TT, Maccarrone M and Corazza GR (2011) The endogenous cannabinoid system in the gut of patients with inflammatory bowel disease. *Mucosal Immunol* **4**:574-583.

Esser N, L'Homme L, De Roover A, Kohnen L, Scheen AJ, Moutschen M, Piette J, Legrand-Poels S and Paquot N (2013) Obesity phenotype is related to NLRP3 inflammasome activity and immunological profile of visceral adipose tissue. *Diabetologia* **56**:2487-2497.

Gatta L, Piscitelli F, Giordano C, Boccella S, Lichtman A, Maione S and Di Marzo V (2012) Discovery of prostamide F2alpha and its role in inflammatory pain and dorsal horn nociceptive neuron hyperexcitability, in *PLoS One* p e31111, United States.

Grishman EK, White PC and Savani RC (2012) Toll-like receptors, the NLRP3 inflammasome, and interleukin-1beta in the development and progression of type 1 diabetes. *Pediatr Res* **71**:626-632.

Han H, Wang Y, Li X, Wang PA, Wei X, Liang W, Ding G, Yu X, Bao C, Zhang Y, Wang Z and Yi F (2013) Novel role of NOD2 in mediating Ca2+ signaling: evidence from NOD2-regulated podocyte TRPC6 channels in hyperhomocysteinemia. *Hypertension* **62**:506-511.

Hegde VL, Hegde S, Cravatt BF, Hofseth LJ, Nagarkatti M and Nagarkatti PS (2008) Attenuation of experimental autoimmune hepatitis by exogenous and endogenous cannabinoids: involvement of regulatory T cells. *Mol Pharmacol* **74**:20-33.

Hernangomez M, Mestre L, Correa FG, Loria F, Mecha M, Inigo PM, Docagne F, Williams RO, Borrell J and Guaza C (2012) CD200-CD200R1 interaction contributes to neuroprotective effects of anandamide on experimentally induced inflammation. *Glia* **60**:1437-1450.

Jackson AR, Nagarkatti P and Nagarkatti M (2014) Anandamide attenuates Th-17 cell-mediated delayed-type hypersensitivity response by triggering IL-10 production and consequent microRNA induction. *PLoS One* **9**:e93954.

Kerr DM, Burke NN, Ford GK, Connor TJ, Harhen B, Egan LJ, Finn DP and Roche M (2012) Pharmacological inhibition of endocannabinoid degradation modulates the expression of inflammatory mediators in the hypothalamus following an immunological stressor. *Neuroscience* **204**:53-63.

Kinsey SG, Naidu PS, Cravatt BF, Dudley DT and Lichtman AH (2011) Fatty acid amide hydrolase blockade attenuates the development of collagen-induced arthritis and related thermal hyperalgesia in mice. *Pharmacology, biochemistry, and behavior* **99**:718-725.

Koda N, Tsutsui Y, Niwa H, Ito S, Woodward DF and Watanabe K (2004) Synthesis of prostaglandin F ethanolamide by prostaglandin F synthase and identification of Bimatoprost as a potent inhibitor of the enzyme: new enzyme assay method using LC/ESI/MS. *Arch Biochem Biophys* **424**:128-136.

Kozak KR, Crews BC, Morrow JD, Wang LH, Ma YH, Weinander R, Jakobsson PJ and Marnett LJ (2002) Metabolism of the endocannabinoids, 2-arachidonylglycerol and anandamide, into prostaglandin, thromboxane, and prostacyclin glycerol esters and ethanolamides. *J Biol Chem* **277**:44877-44885.

Krustev E, Reid A and McDougall JJ (2014) Tapping into the endocannabinoid system to ameliorate acute inflammatory flares and associated pain in mouse knee joints. *Arthritis Res Ther* **16**:437.

Lara-Celador I, Castro-Ortega L, Alvarez A, Goni-de-Cerio F, Lacalle J and Hilario E (2012) Endocannabinoids reduce cerebral damage after hypoxic-ischemic injury in perinatal rats. *Brain Res* **1474**:91-99.

Lee HM, Kim JJ, Kim HJ, Shong M, Ku BJ and Jo EK (2013) Upregulated NLRP3 inflammasome activation in patients with type 2 diabetes. *Diabetes* **62**:194-204.

Lemieux LI, Rahal SS and Kennedy CR (2003) PGE2 reduces arachidonic acid release in murine podocytes: evidence for an autocrine feedback loop. *Am J Physiol Cell Physiol* **284**:C302-309.

Li C, Xia M, Abais JM, Liu X, Li N, Boini KM and Li PL (2013) Protective role of growth hormone against hyperhomocysteinemia-induced glomerular injury. *Naunyn Schmiedebergs Arch Pharmacol* **386**:551-561.

Martinon F and Tschopp J (2005) NLRs join TLRs as innate sensors of pathogens. *Trends Immunol* **26**:447-454.

Masters SL, Dunne A, Subramanian SL, Hull RL, Tannahill GM, Sharp FA, Becker C, Franchi L, Yoshihara E, Chen Z, Mullooly N, Mielke LA, Harris J, Coll RC, Mills KH, Mok KH, Newsholme P, Nunez G, Yodoi J, Kahn SE, Lavelle EC and O'Neill LA (2010) Activation of the NLRP3 inflammasome by islet amyloid polypeptide provides a mechanism for enhanced IL-1beta in type 2 diabetes. *Nat Immunol* **11**:897-904.

McLean RR, Jacques PF, Selhub J, Tucker KL, Samelson EJ, Broe KE, Hannan MT, Cupples LA and Kiel DP (2004) Homocysteine as a predictive factor for hip fracture in older persons, in *N Engl J Med* pp 2042-2049, 2004 Massachusetts Medical Society, United States.

Mestre L, Correa F, Arevalo-Martin A, Molina-Holgado E, Valenti M, Ortar G, Di Marzo V and Guaza C (2005) Pharmacological modulation of the endocannabinoid system in a viral model of multiple sclerosis. *J Neurochem* **92**:1327-1339.

Mukhopadhyay P, Pan H, Rajesh M, Batkai S, Patel V, Harvey-White J, Mukhopadhyay B, Hasko G, Gao B, Mackie K and Pacher P (2010a) CB1 cannabinoid receptors promote oxidative/nitrosative stress, inflammation and cell death in a murine nephropathy model. *Br J Pharmacol* **160**:657-668.

Mukhopadhyay P, Rajesh M, Pan H, Patel V, Mukhopadhyay B, Batkai S, Gao B, Hasko G and Pacher P (2010b) Cannabinoid-2 receptor limits inflammation, oxidative/nitrosative stress, and cell death in nephropathy. *Free Radic Biol Med* **48**:457-467.

Murphy N, Cowley TR, Blau CW, Dempsey CN, Noonan J, Gowran A, Tanveer R, Olango WM, Finn DP, Campbell VA and Lynch MA (2012) The fatty acid amide hydrolase inhibitor

URB597 exerts anti-inflammatory effects in hippocampus of aged rats and restores an age-related deficit in long-term potentiation. *J Neuroinflammation* **9**:79.

Naidu PS, Kinsey SG, Guo TL, Cravatt BF and Lichtman AH (2010) Regulation of inflammatory pain by inhibition of fatty acid amide hydrolase. *J Pharmacol Exp Ther* **334**:182-190.

Nicotra LL, Vu M, Harvey BS and Smid SD (2013) Prostaglandin ethanolamides attenuate damage in a human explant colitis model. *Prostaglandins Other Lipid Mediat* **100-101**:22-29.

Peeters PM, Eurlings IM, Perkins TN, Wouters EF, Schins RP, Borm PJ, Drommer W, Reynaert NL and Albrecht C (2014) Silica-induced NLRP3 inflammasome activation in vitro and in rat lungs. *Part Fibre Toxicol* **11**:58.

Peeters PM, Perkins TN, Wouters EF, Mossman BT and Reynaert NL (2013) Silica induces NLRP3 inflammasome activation in human lung epithelial cells. *Part Fibre Toxicol* **10**:3.

Perla-Kajan J and Jakubowski H (2012) Paraoxonase 1 and homocysteine metabolism. *Amino Acids* **43**:1405-1417.

Raij L, Azar S and Keane W (1984) Mesangial immune injury, hypertension, and progressive glomerular damage in Dahl rats. *Kidney Int* **26**:137-143.

Ravaglia G, Forti P, Maioli F, Martelli M, Servadei L, Brunetti N, Porcellini E and Licastro F (2005) Homocysteine and folate as risk factors for dementia and Alzheimer disease. *Am J Clin Nutr* **82**:636-643.

Rettori E, De Laurentiis A, Zorrilla Zubilete M, Rettori V and Elverdin JC (2012) Anti-inflammatory effect of the endocannabinoid anandamide in experimental periodontitis and stress in the rat. *Neuroimmunomodulation* **19**:293-303.

Ritter JK, Li C, Xia M, Poklis JL, Lichtman AH, Abdullah RA, Dewey WL and Li PL (2012) Production and actions of the anandamide metabolite prostamide E2 in the renal medulla. *J Pharmacol Exp Ther* **342**:770-779.

Salaga M, Mokrowiecka A, Zakrzewski PK, Cygankiewicz A, Leishman E, Sobczak M, Zatorski H, Malecka-Panas E, Kordek R, Storr M, Krajewska WM, Bradshaw HB and Fichna J (2014) Experimental colitis in mice is attenuated by changes in the levels of endocannabinoid metabolites induced by selective inhibition of fatty acid amide hydrolase (FAAH). *Journal of Crohn's & colitis* **8**:998-1009.

Sasso O, Bertorelli R, Bandiera T, Scarpelli R, Colombano G, Armirotti A, Moreno-Sanz G, Reggiani A and Piomelli D (2012) Peripheral FAAH inhibition causes profound antinociception and protects against indomethacin-induced gastric lesions. *Pharmacological research* **65**:553-563.

Schuelert N, Johnson MP, Oskins JL, Jassal K, Chambers MG and McDougall JJ (2011) Local application of the endocannabinoid hydrolysis inhibitor URB597 reduces nociception in spontaneous and chemically induced models of osteoarthritis. *Pain* **152**:975-981.

Sutterwala FS, Ogura Y and Flavell RA (2007) The inflammasome in pathogen recognition and inflammation. *J Leukoc Biol* **82**:259-264.

Tchantchou F, Tucker LB, Fu AH, Bluett RJ, McCabe JT, Patel S and Zhang Y (2014) The fatty acid amide hydrolase inhibitor PF-3845 promotes neuronal survival, attenuates inflammation and improves functional recovery in mice with traumatic brain injury. *Neuropharmacology* **85**:427-439.

Turcotte C, Chouinard F, Lefebvre JS and Flamand N (2015) Regulation of inflammation by cannabinoids, the endocannabinoids 2-arachidonoyl-glycerol and arachidonoyl-ethanolamide, and their metabolites. *J Leukoc Biol* **97**:1049-1070.

Vercelli CA, Aisemberg J, Billi S, Cervini M, Ribeiro ML, Farina M and Franchi AM (2009) Anandamide regulates lipopolysaccharide-induced nitric oxide synthesis and tissue damage in the murine uterus. *Reprod Biomed Online* **18**:824-831.

Wang X, Chrysovergis K, Kosak J and Eling TE (2014) Lower NLRP3 inflammasome activity in NAG-1 transgenic mice is linked to a resistance to obesity and increased insulin sensitivity. *Obesity (Silver Spring)* **22**:1256-1263.

Wang ZY, Wang P, Hillard CJ and Bjorling DE (2015) Attenuation of cystitis and pain sensation in mice lacking fatty acid amide hydrolase. *J Mol Neurosci* **55**:968-976.

Wree A, Eguchi A, McGeough MD, Pena CA, Johnson CD, Canbay A, Hoffman HM and Feldstein AE (2014) NLRP3 inflammasome activation results in hepatocyte pyroptosis, liver inflammation, and fibrosis in mice. *Hepatology* **59**:898-910.

Wu CC, Zheng CM, Lin YF, Lo L, Liao MT and Lu KC (2012) Role of homocysteine in end-stage renal disease. *Clin Biochem* **45**:1286-1294.

Xia M, Conley SM, Li G, Li PL and Boini KM (2014) Inhibition of hyperhomocysteinemia-induced inflammasome activation and glomerular sclerosis by NLRP3 gene deletion. *Cell Physiol Biochem* **34**:829-841.

Yang W, Ni J, Woodward DF, Tang-Liu DD and Ling KH (2005) Enzymatic formation of prostamide F2alpha from anandamide involves a newly identified intermediate metabolite, prostamide H2. *J Lipid Res* **46**:2745-2751.

Yi F, dos Santos EA, Xia M, Chen QZ, Li PL and Li N (2007) Podocyte injury and glomerulosclerosis in hyperhomocysteinemic rats. *Am J Nephrol* **27**:262-268.

Yu M, Ives D and Ramesha CS (1997) Synthesis of prostaglandin E2 ethanolamide from anandamide by cyclooxygenase-2. *J Biol Chem* **272**:21181-21186.

Yu M, Sturgill-Short G, Ganapathy P, Tawfik A, Peachey NS and Smith SB (2012) Age-related changes in visual function in cystathionine-beta-synthase mutant mice, a model of hyperhomocysteinemia, in *Exp Eye Res* pp 124-131, A 2011. Published by Elsevier Ltd., England.

Zhang C, Boini KM, Xia M, Abais JM, Li X, Liu Q and Li PL (2012) Activation of Nod-like receptor protein 3 inflammasomes turns on podocyte injury and glomerular sclerosis in hyperhomocysteinemia. *Hypertension* **60**:154-162.

Zhang C, Hu JJ, Xia M, Boini KM, Brimson C and Li PL (2010) Redox signaling via lipid raft clustering in homocysteine-induced injury of podocytes. *Biochim Biophys Acta* **1803**:482-491.

Zheng BJ, Chan KW, Lin YP, Zhao GY, Chan C, Zhang HJ, Chen HL, Wong SS, Lau SK, Woo PC, Chan KH, Jin DY and Yuen KY (2008) Delayed antiviral plus immunomodulator treatment still reduces mortality in mice infected by high inoculum of influenza A/H5N1 virus. *Proc Natl Acad Sci U S A* **105**:8091-8096.

24

Footnotes

[1]These authors contributed equally to this work.

FIGURE LEGENDS

Figure 1. Protective Action of AEA at Different Concentrations against Hcys-induced NLRP3 Inflammasome Activation and Podocyte Injury via Its COX-2 Metabolites. Podocytes were cultured for 24 hrs with 40 µM L-homocysteine (Hcys) in the absence (vehicle only, Vehl) or presence of increasing anandamide (AEA) concentrations as indicated. In one group, the cells were co-treated with celecoxib (CEL) (1 µM). A. Caspase-1 activity in different groups of podocytes (n=6). B. IL-1β production in different groups of podocytes (n=6). C. Vascular endothelial growth factor (VEGF) production in different groups of podocytes (n=6). * $p < 0.05$ vs. Ctrl group, # $p < 0.05$ vs. Vehl-Hcys group. & $p < 0.05$ vs. AEA 100 µM-Hcys group.

Figure 2. COX-2-dependent Protection of Glomerular Podocytes by AEA against hHcys-induced NLRP3 Inflammasome Formation and Activation in Mice. A. Images showing the colocalization between NLRP3 (green) with ASC (red) in glomeruli of mice receiving either normal diet (ND) or folate-free (FF) diet and the different treatments shown with summarized data (n=6). B. Images showing the colocalization between NLRP3 (green) with caspase-1 (red) in glomeruli from different groups and summarized data (n=6). C. Images showing IL-1β immunoreactivity in glomeruli from different groups of mice and summarized data (n=6). * $p < 0.05$ vs. WT-Vehl-ND group, # $p < 0.05$ vs. WT-Vehl-FF group.

Figure 3. Prevention by AEA of hHcys-induced Glomerular Damage in Mice. A. Summarized data showing the urinary protein excretion rate from different groups of mice (n=6). B. Summarized data showing the urine albumin excretion rate from different groups of mice

(n=6). C. Images showing the glomerular morphological changes from different groups of mice and summarized data (n=6). * $p < 0.05$ vs. WT-Vehl-ND group, # $p < 0.05$ vs. WT-Vehl-FF group.

Figure 4. Amelioration by AEA of hHcys-induced Podocyte Injury in Mice. A. Images showing immunostained glomeruli for podocin from different groups of mice. B. Images showing immunostained glomeruli for desmin from different groups of mice. C. Summarized data for podocin (left) and desmin (right) (n=6). * $p < 0.05$ vs. WT-Vehl-ND group, # $p < 0.05$ vs. WT-Vehl-FF group.

Figure 5. Inhibition of Hcys-induced NLRP3 Inflammasome Formation by PGE2-EA in Podocytes. Podocytes were cultured for 24 hrs with Hcys (40 µM) in the absence or presence of PGE2-EA (10 µM) or AEA (10 µM). A. Images showing colocalization of NLRP3 (Alexa 488, green color) with ASC (Alexa 555, red color) in podocytes and summarized data showing the fold changes in Pearson correlation coefficient for the colocalization of NLRP3 with ASC (n=6). B. Images showing colocalization of Nlrp3 (Alexa 488, green color) with Casp (Alexa 555, red color) in podocytes and summarized data showing the fold changes in correlation coefficient for the colocalization of NLRP3 with Casp (n=6). * $p < 0.05$ vs. Ctrl. # $p < 0.05$ *vs*. corresponded Hcys group.

Figure 6. **Blockade by PGE2-EA of Hcys-induced NLRP3 Inflammasome Activation in Podocytes.** A. Caspase-1 activity in different groups of podocytes (n=6). B. IL-1β production in different groups of podocytes (n=6). * $p < 0.05$ vs. Ctrl group; # $p < 0.05$ vs. Vehl-Hcys group.

27

Figure 7. Protective Effect of PGE2-EA against Hcys-induced Podocyte Injury. A. Images showing the expression of F-actin fiber in different groups of control or treated podocytes and summarized data (n=6). B. Summarized data showing production of VEGF in different groups of podocytes (n=6). * $p < 0.05$ vs. Ctrl group; # $p < 0.05$ vs. Vehl-Hcys group.

Figure 8. Protective Effect of PGE2-EA against Hcys-induced Podocyte Injury. A. Images showing the expression of podocin in different groups of podocytes and summarized data (n=6). B. Images showing the expression of desmin in different groups of podocytes and summarized data (n=6). * $p < 0.05$ vs. Ctrl group; # $p < 0.05$ vs. Vehl-Hcys group.
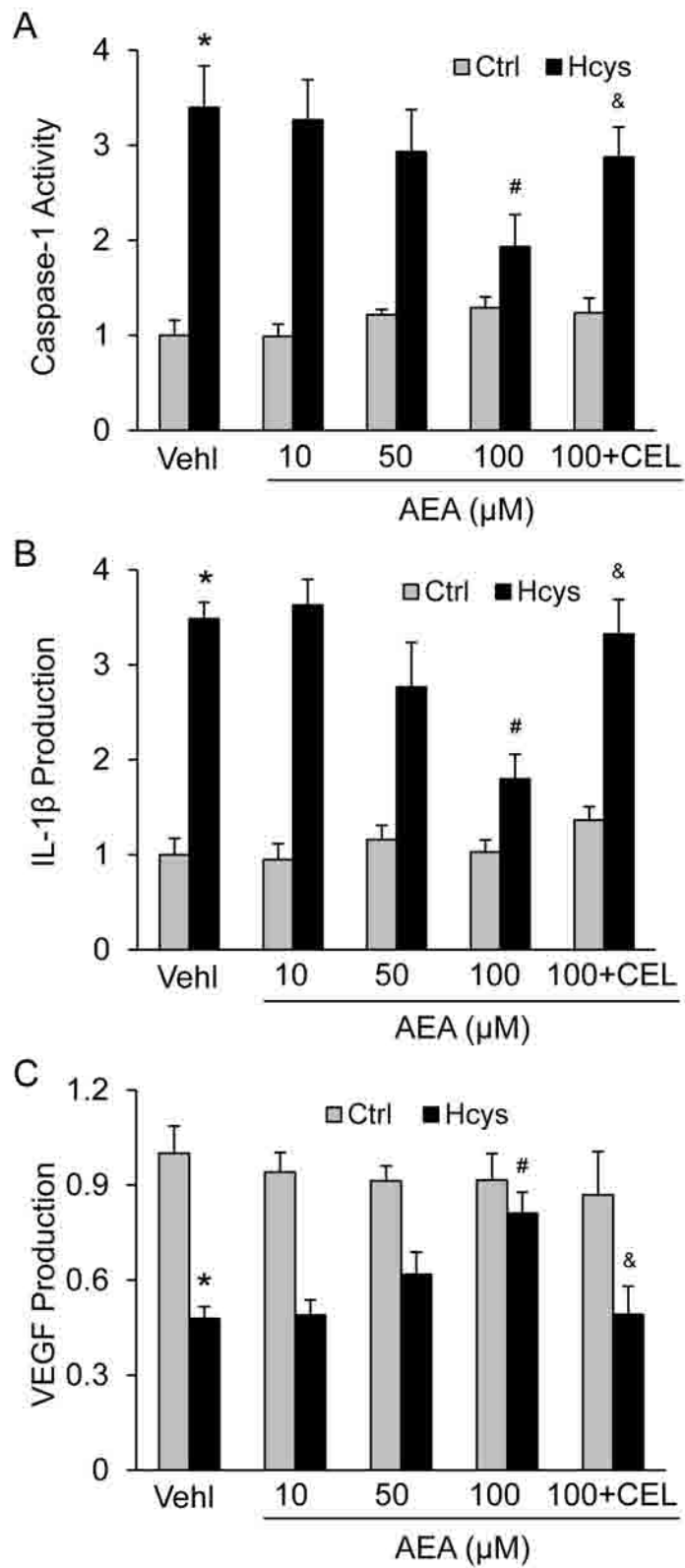
Fig. 1
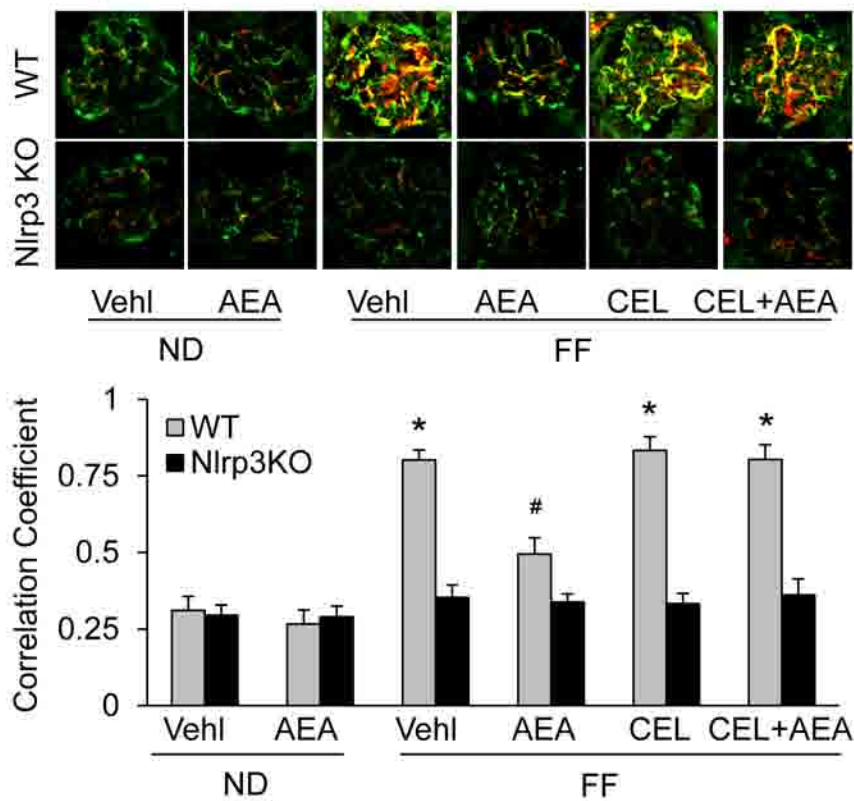
Fig. 2A

B **Nlrp3** vs **Caspase-1**

WT

Nlrp3 KO

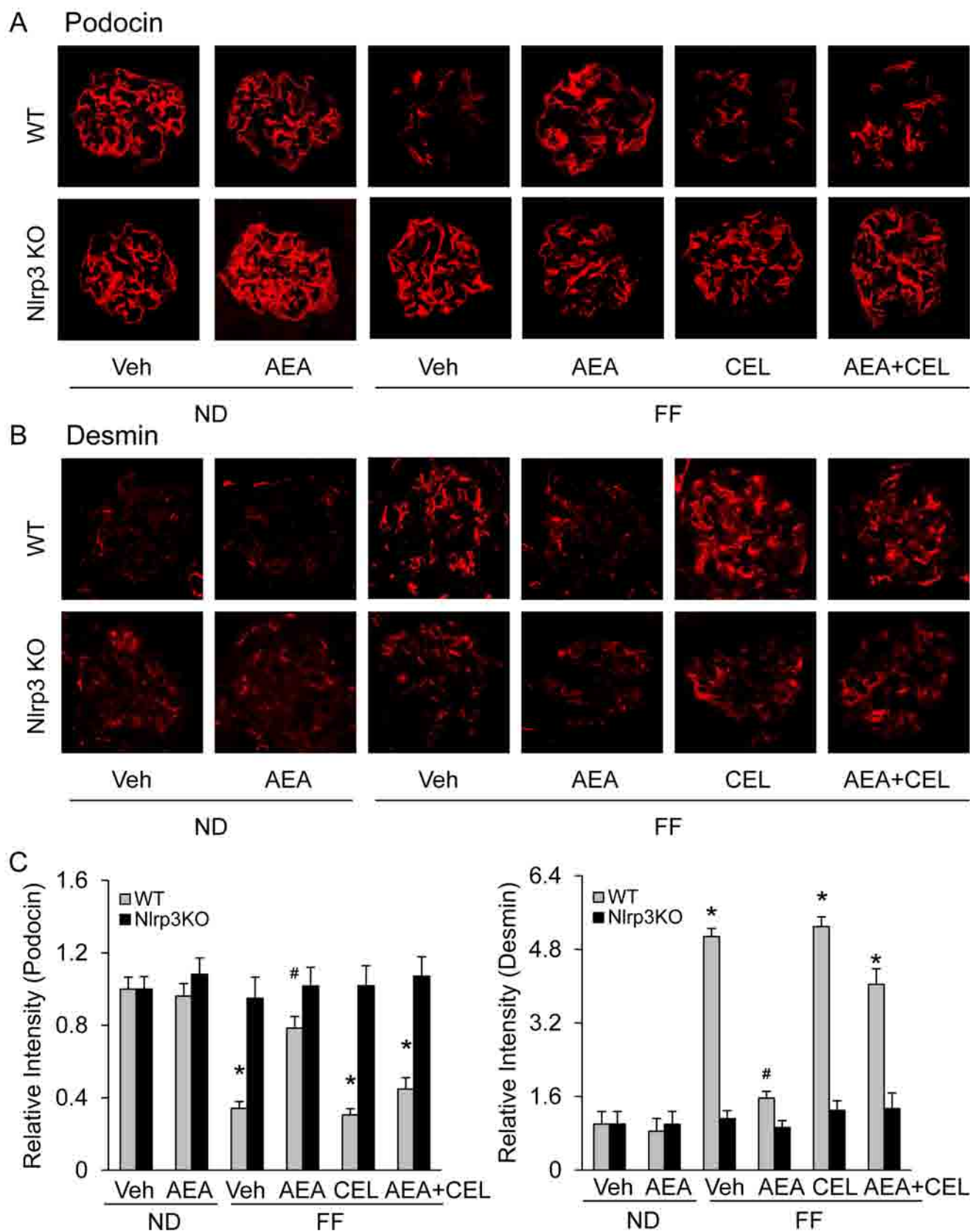| Vehl	AEA	Vehl	AEA	CEL	CEL+AEA
ND		FF			

Fig. 2B

C   IL-1β Stain

Fig. 2C

Fig. 3

A Podocin

WT

Nlrp3 KO

Veh · AEA

ND

Veh · AEA · CEL · AEA+CEL

FF

B Desmin

WT

Nlrp3 KO

Veh · AEA

ND

Veh · AEA · CEL · AEA+CEL

FF

C

Relative Intensity (Podocin)

☐ WT
■ Nlrp3KO

Veh AEA | Veh AEA CEL AEA+CEL
ND | FF

Relative Intensity (Desmin)

☐ WT
■ Nlrp3KO

Veh AEA | Veh AEA CEL AEA+CEL
ND | FF

Fig. 4

Fig. 5

Fig. 6

Fig. 7

A Podocin

Ctrl

Hcys

Vehl   PE2   AEA

B Desmin

Ctrl

Hcys

Vehl   PE2   AEA

Fig. 8